DELPHI Collaboration

DELPHI-2000-030 CONF 349
6 March, 2000

Search for neutralino pair production at $\sqrt{s} = 189$ GeV

DELPHI Collaboration

PRELIMINARY RESULTS

P. Andersson [1], **M. Espirito Santo**[2], **K. Hultqvist** [1], **A. Lipniacka** [1], **F. Mazzucato** [3], **J. Strandberg** [1]

Abstract

A search for pair-production of neutralinos at a LEP centre-of-mass energy of 189 GeV has been performed. No signal was found and limits on the neutralino production cross-section at 95 % confidence level were obtained. These limits have been used to exclude regions in the parameter space of the MSSM.

Submitted to the XXXVth Rencontre de Moriond, "Electroweak interactions and unified theories", March 2000.

[1] Fysikum, Stockholm University, Box 6730, S-113 85 Stockholm, Sweden

[2] CERN, CH-1211 Genève 23, Switzerland

[3] Dipartimento di Fisica, Universita di Padova, Via Marzolo 8, Padova, Italy

1 Introduction

During 1998, the DELPHI experiment at LEP accumulated an integrated luminosity of 158 pb^{-1} at a centre-of-mass energy of 188.7 GeV. Preliminary results of a search for neutralino pair production in these data are reported here. In a separate note [1], these results are interpreted together with those of other DELPHI searches to set mass limits on neutralinos, sleptons and charginos.

In the Minimal Supersymmetric Standard Model (the MSSM)[2], there are four neutralinos $\tilde{\chi}_i^0, i = 1,4$, numbered in order of increasing mass, and two charginos $\tilde{\chi}_j^{\pm}, j = 1,2$. These are linear combinations of the supersymmetric (SUSY) partners of neutral and charged gauge and Higgs bosons. In the following, R-parity conservation is assumed, implying a stable lightest supersymmetric particle (LSP), which is assumed to be $\tilde{\chi}_1^0$. R-parity conservation also implies pair-production of SUSY particles, each decaying (directly or indirectly) into a $\tilde{\chi}_1^0$ which is weakly interacting and escapes detection, giving a signature of missing energy and momentum.

The neutralinos can be pair-produced at LEP2 via s-channel Z exchange or t-channel exchange of a scalar electron (selectron, $\tilde{\mathrm{e}}$). The decay of heavier neutralino states to lighter ones involves emission of either a fermion-antifermion pair or a photon. If the scalar leptons (sleptons) are light the leptonic decays may be enhanced by slepton exchange, and the two-body decay $\tilde{\chi}_i^0 \to \tilde{\ell}\overline{\ell}$ (followed by $\tilde{\ell} \to \tilde{\chi}_j^0 \ell$) may dominate. Decays via charginos are also possible.

Of the detectable channels (*i.e.* excluding $\tilde{\chi}_1^0\tilde{\chi}_1^0$), $\tilde{\chi}_1^0\tilde{\chi}_2^0$ and $\tilde{\chi}_1^0\tilde{\chi}_3^0$ are important for large regions in the parameter space. For a more complete coverage, however, one must also consider channels like $\tilde{\chi}_2^0\tilde{\chi}_3^0$ and $\tilde{\chi}_2^0\tilde{\chi}_4^0$, giving cascade decays with multiple jets or leptons in the final state. Moreover, a light scalar tau lepton (stau) is likely to arise because of left-right mixing of the stau states. For $M_{\tilde{\tau}_1}$ close to $M_{\tilde{\chi}_1^0}$ the search for direct chargino production fails since the decay $\tilde{\chi}_1^{\pm} \to \tilde{\tau}_1\nu$, followed by the decay of $\tilde{\tau}_1$ into a neutralino and a low energy τ, dominates. In this case the $\tilde{\chi}_1^0\tilde{\chi}_2^0$ and $\tilde{\chi}_2^0\tilde{\chi}_2^0$ channels with the decay $\tilde{\chi}_2^0 \to \tilde{\chi}_1^0\tau\bar{\tau}$ which proceedes via an intermediate stau and gives two taus with different energy, become important.

The search for neutralino production in the $\mathrm{q\bar{q}}$ and $\ell^+\ell^-$ visible final states, from $\tilde{\chi}_k^0\tilde{\chi}_1^0$ production with $\tilde{\chi}_k^0 \to \tilde{\chi}_1^0 + \mathrm{f\bar{f}}$, applied the methods described in Refs. [3, 4] with minor changes. In addition, several new searches were introduced in order to obtain a more complete coverage, in particular to allow setting a limit on $M_{\tilde{\chi}_1^0}$:

- A search for multijet events, as from $\tilde{\chi}_i^0\tilde{\chi}_j^0, i = 1,2, j = 3,4$ with $\tilde{\chi}_j^0 \to \tilde{\chi}_2^0\mathrm{q\bar{q}}$ and $\tilde{\chi}_2^0$ decaying to $\tilde{\chi}_1^0\mathrm{q\bar{q}}$ or $\tilde{\chi}_1^0\gamma$.

- A search for multilepton events for the corresponding decays to lepton pairs.

- A search for events with low transverse energy and low multiplicity, e.g. arising from $\tilde{\chi}_2^0\tilde{\chi}_2^0$ production with $\tilde{\chi}_2^0 \to \tilde{\chi}_1^0\ell^+\ell^-$and low $M_{\tilde{\chi}_2^0}$-$M_{\tilde{\chi}_1^0}$, or from neutralino decays via intermediate slepton states.

- A search for cascade decays with tau leptons, e.g. $\tilde{\chi}_2^0\tilde{\chi}_1^0$ production with $\tilde{\chi}_2^0 \to \tilde{\tau}\tau$ and $\tilde{\tau} \to \tilde{\chi}_1^0\tau$ (see also [5]).

No excess over the expected Standard Model background was found and the results were used to place limits on the cross-section for neutralino pair production. In addition,

limits were set within the MSSM scheme with universal parameters at the high mass scale typical of Grand Unified Theories [2].

The DELPHI detector has been described elsewhere [6]. It consists of a central tracking system, where the main component is a Time Projection Chamber (TPC), supplemented by a system of silicon tracking detectors and drift chambers. The electromagnetic calorimeters are symmetric around the plane perpendicular to the beam (θ=90°), with the High density Projection Chamber (HPC) extending from 88.7° to 43.1°, the Forward Electromagnetic Calorimeter (FEMC) from 35° down to 8°, overlapping with the Small angle Tile Calorimeter (STIC), which covers the range $10.6° > \theta > 1.7°$. The region of weak electromagnetic calorimetry at a polar angle close to 40° is instrumented by scintillators (hermeticity taggers) which serve to reject events with unmeasured photons.

2 Data samples and event generators

The total integrated luminosity collected by DELPHI during 1998 at E_{cm} = 188.7 GeV was 158 pb^{-1}, with 153 pb^{-1}of adequate data quality to be used in the present searches.

To evaluate the signal efficiencies and background contaminations, events were generated using several different programs. All relied on `JETSET` 7.4 [7], tuned to LEP 1 data [8], for quark fragmentation.

`SUSYGEN 2.2004`[9] was used to generate neutralino signal events and calculate cross-sections and branching ratios.

The background process $e^+e^- \to q\bar{q}(n\gamma)$ was generated with `PYTHIA 5.7` [7]. For $\mu^+\mu^-(\gamma)$ and $\tau^+\tau^-(\gamma)$, `DYMU3` [10] and `KORALZ 4.2` [11] were used, respectively, while the generator of Ref. [12] was used for $e^+e^- \to e^+e^-$ events. Production of four-fermion final states was generated using `EXCALIBUR`[13] and `grc4f`[14].

Two-photon interactions giving hadronic final states were generated using `TWOGAM`[15], and `PHOJET`[16].

The generated signal and background events were passed through the detailed simulation of the DELPHI detector [6] and then processed with the same reconstruction and analysis programs as the real data. The numbers of simulated events from different background processes were several times the numbers in the real data.

In addition, the fast detector simulation SGV[17], tuned for the present selections, was used in order to estimate efficiencies for points without full simulation, and to take into account all contributing production and decay channels for a given point in the MSSM parameter space. The efficiencies were checked to typically agree within 10% relative with those obtained by full simulation.

Figures 1 and 2 show the expected distribution for some relevant event variables for $\tilde{\chi}_1^0\tilde{\chi}_2^0$ production as obtained using the full detector simulation and SGV.

Figures 3, 4, 5 show comparison between real and simulated events at various steps of the selections described in the following sections.

3 Event selection

The different searches used were designed to be mutually exclusive, in order to allow easy combination of the results. Jets were reconstructed using the LUCLUS algorithm [7] with d_{join} = 10 GeV/c. All searches made use of the information from the hermeticity taggers

to reject events with photons from initial state radiation lost in the otherwise insensitive region at polar angles around 40° and 140°. Events were rejected if there were active taggers in the direction of the missing momentum and not associated to reconstructed jets. Leptons were identified using the standard DELPHI "loose tag" criteria[6], except for electrons in the acoplanar leptons search (see section 3.2).

3.1 Acoplanar jets search

Earlier variations of this search have been described in Refs. [4, 3].

At least five well reconstructed charged particles were required, including one with a transverse momentum above 1.5 GeV/c. The sum of the moduli of momenta of well reconstructed charged particles had to be greater than 4 GeV/c, and the transverse energy had to exceed 4 GeV. Two jets were required, each satisfying $10° < \theta_{jet} < 170°$, and containing at least one well reconstructed charged particle. Tracks which were badly reconstructed, or did not originate from the interaction point, were required not to carry more than 45% of the visible energy ($E_{\rm vis}$), and their associated calorimeter energy had to be less than 20% of $E_{\rm vis}$.

To reject two-photon events several criteria were used. The fraction of the total energy carried by particles emitted within 30° of the beam had to be less than 60%, the polar angle of the total momentum had to satisfy $|\cos\theta_p| < 0.9$, and the transverse momentum had to exceed 6 GeV/c. Figure 3(a) shows the distributions of invariant mass of the visible system ($M_{\rm vis}$) divided by $\sqrt{s}$, for real and simulated events passing the above selection.

Events were also rejected if there was a neutral particle, either with an energy above 60 GeV, or isolated from the nearest jet by at least 20°, and with an energy above 20 GeV. These criteria served to reject Zγ events.

To reject WW background no charged particle with momentum above 20 GeV/c was allowed, and the most isolated electron or muon (if any) had to be within 20° of the nearest jet and have a momentum below 10 GeV/c. Figure 3(c) shows the distributions of transverse momentum ($p_{\rm T}$) divided by $\sqrt{s}$ for real and simulated data, following the above selection.

In the last step of the selection, criteria optimised for different neutralino mass differences (ΔM) were applied in logical OR. These involved the transverse momentum ($p_{\rm T}$), longitudinal momentum ($p_{\rm L}$), and invariant mass ($M_{\rm vis}$) of the visible system, as well as the mass recoiling against it ($M_{\rm rec}$). Also the scaled acoplanarity (the acoplanarity of the two jets multiplied by the sine of the minimum angle between a jet and the beam axis) and the acollinearity of the two jets were used in this step:

- For low ΔM ($\sim$10 GeV/c^2) it was required that $M_{\rm vis} < 0.1\sqrt{s}/c^2$, $M_{\rm rec} > 0.7\sqrt{s}/c^2$, and $p_{\rm T} > 7$ GeV/c. In addition, the scaled acoplanarity was required to exceed 40°.

- For intermediate ΔM ($\sim$40 GeV/c^2) it was required that $0.1\sqrt{s}/c^2 < M_{\rm vis} < 0.3\sqrt{s}/c^2$, $M_{\rm rec} > 0.6\sqrt{s}/c^2$, and $p_{\rm T} > 8$ GeV/c. The scaled acoplanarity had to exceed 25°.

- For high ΔM ($\sim$90 GeV/c^2) it was required that $0.3\sqrt{s}/c^2 < M_{\rm vis} < 0.5\sqrt{s}/c^2$, $M_{\rm rec} > 0.45\sqrt{s}/c^2$, 12 GeV/$c < p_{\rm T} <$ 35 GeV/c, and also that $p_{\rm L} <$ 35 GeV/c. The scaled acoplanarity had to exceed 25°, and the acollinearity had to be below 55°.

Figure 3 (e) shows a comparison of the scaled acoplanarity for the real and simulated data events passing the last step of the selection.

3.2 Acoplanar leptons search

The search for acoplanar leptons selects events with exactly two isolated oppositely charged particles (lepton candidates) with momentum above 1 GeV/c, and at most five charged particles in total. This search was slightly modified with respect to Ref. [3], as follows. The minimum number of TPC pad rows required for the two selected charged particles was increased from four to five. The lepton identification requirements were changed, accepting as electrons those particles which had an associated energy in the electromagnetic calorimeter exceeding half of the measured momentum, while for muons the "loose tag"[6] was used. Either both particles in the pair were required to be selected electrons, not simultaneously identified as muons, or else both particles had to be muons. In addition to the acoplanarity, the acollinearity between the two particles was also required to exceed 10°. The minimum transverse momentum was increased from 5 to 6 GeV/c, and the maximum accepted energy in the STIC was reduced from 1 to 0.3 GeV. To improve the rejection of WW background events with missing momentum above 45 GeV/c, and a scalar sum of the momenta of the two selected particles in excess of 100 GeV/c, were rejected. As before, three sets of criteria optimised for different ΔM ranges were used in logical OR. These criteria were unchanged, except for the minimal missing mass required in the case of large ΔM which was changed from $0.4\sqrt{s}/c^2$ to $0.2\sqrt{s}/c^2$.

Figure 3 (b,d,f) shows a comparison between real and simulated data; for events passing the initial step of the above selection corresponding to rejection of bhabha events (b), the intermediate step corresponding to rejection of two-photon events (d), and the last step (f).

3.3 Multijet search

The multijet search was optimised for cascade decays of neutralinos with large mass splittings, giving high energy jets. Events with energetic photons, characteristic of the decay $\tilde{\chi}^0_2 \to \tilde{\chi}^0_1\gamma$, were subjected to less stringent selection criteria, giving a separate set of selected events with low background and comparatively high efficiency.

At least five well-reconstructed charged particles were required, and at least one of these had to have a transverse momentum exceeding 2.5 GeV/c. The transverse energy of the event had to be greater than 25 GeV, and the energy of tracks which were badly reconstructed or did not originate from the interaction point was required to be less than 30 GeV and less than 45% of the visible energy. In addition, the calorimeter energy associated to such tracks had to be less than 20% of $E_{\rm vis}$. Figure 4 (a) shows the distributions of $M_{\rm vis}$ divided by the centre-of-mass energy for real data and simulated background events passing the above selection.

The total energy in the electromagnetic calorimeters had to be less than 70 GeV, and there had to be no single calorimeter shower above 60 GeV. The energy carried by particles within 30° of the beam had to be less than 60% of the visible energy. The total visible energy had to be less than 135 GeV, the polar angle of the total momentum had to satisfy $|\cos\theta_p| < 0.9$, and the transverse momentum had to exceed 6 GeV/c. Figure 4

(c) gives a comparison of the $p_{\rm T}/\sqrt{s}$-distributions for real data and simulated background following the above selection.

The scaled acoplanarity (see section 3.1), forcing two jets to be reconstructed, had to be greater than 10°. The polar angle of the most energetic jet had to be outside the range between 85° and 95°, and its energy had to be less than 56 GeV.

To reject WW background it was required that there be no charged particle with a momentum above 30 GeV/c, and that the momentum of the most isolated electron or muon (if any) be below 10 GeV/c, or below 4 GeV/c if the angle between the lepton and the nearest jet was greater than 20°.

Events with a photon signature were then selected on the basis of reconstructed photons in the polar angle range between 20° and 160°, isolated by more than 20° from the nearest charged track. At least two such photons with energies above 10 GeV were required, or one photon with energy above 10 GeV and below 40 GeV.

For the complementary sample, without a photon signature, two additional requirements were imposed to reject Zγ events: the mass recoiling against the system of visible particles had to be greater than 100 GeV/c^2, and all jets with energy above 20 GeV had to have a ratio of energy in charged particles to energy in neutral particles which was above 0.15.

Lastly, events selected by the searches for acoplanar leptons or jets (sections 3.2 and 3.1) were rejected. Figure 4 (e) shows the acoplanarity distributions for real and simulated events, without a photon signature, passing the last step of the selection.

3.4 Multilepton search

The multilepton search is sensitive to cascade decays involving leptons, which can dominate if there are light sleptons.

The first step in the selection was in common with the tau cascade search and the low E_T search (sections 3.5 and 3.6). The number of charged particles was required to be at least two and at most eight, and events with more than four neutral particles were rejected. The reconstructed invariant mass had to be below 120 GeV/c^2, and the recoil mass above 20 GeV/c^2. The calorimeter energy associated to particles which were badly reconstructed or did not originate at the vertex, $E_{\rm bc}$, was required not to exceed 0.4 $E_{\rm vis}$, while the energy of well reconstructed charged particles had to be greater than 0.2 $E_{\rm vis}$. It was also required that $E_{\rm vis}+E_{\rm bc}<140$ GeV.

In the following step, at least two charged particles were required to be identified leptons. Figure 4 (b) shows a comparison between $M_{\rm vis}/\sqrt{s}$ distributions for real and simulated events passing the above selection.

To reject Zγ, two-photon, and Bhabha events, it was required that the transverse momentum of the event exceeded 8 GeV/c, and the polar angle of the total momentum was required to satisfy $|\cos\theta_p| < 0.9$. The transverse energy of the event had to be greater than 25 GeV, and the energy in the STIC was required to be less than 10 GeV. The distributions of $p_{\rm T}/\sqrt{s}$ for real and simulated data, following the above selection, are compared in figure 4.

For events with exactly two isolated well-reconstructed charged particles the following requirements were imposed. The acoplanarity and acollinearity for these two particles had to exceed 15° and 6°, respectively. If the total energy in electromagnetic calorimeters exceeded 50 GeV the acollinearity was required to be greater than 10°. To reject two-

lepton background from leptonic decays of W pairs, charge asymmetry was used, requiring the product of charge and cosine of polar angle to be less than -0.1 for the two most energetic charged particles in the event.

For events with two reconstructed jets the scaled acoplanarity (see section 3.1) was required to be greater than 15°.

Lastly, events selected by the searches for acoplanar leptons or jets (sections 3.2 and 3.1) were rejected. Figure 4 (f) shows the distributions of acoplanarity for real and simulated data, following the above selection.

3.5 Tau cascade search

The first step of the selection was the same as for the multilepton (section 3.4), with the additional requirement of no more than two reconstructed jets. Two or more of the charged particles also had to satisfy stricter criteria on reconstruction and impact parameters.

In the next step, the highest and second highest momenta of charged particles were required to be below 50 and 25 GeV/c, respectively and at least one charged particle had to have a transverse momentum above 2.5 GeV/c. Events with neutral showers within 20° of the beam axis were rejected. The visible mass distributions, for real and simulated data at this stage of the selection, are compared in figure 5 (a).

The criteria to reject Zγ, two-photon, and Bhabha events, were the same as for the multilepton search (section 3.4), except for the minimum transverse momentum which was reduced to 7 GeV/c, and the removal of the transverse energy requirement. Figure 5 (c) shows distributions of $E_{\rm vis}/\sqrt{s}$ as a comparison between real and simulated data, selected with the above criteria.

Events with exactly two isolated, well-reconstructed, oppositely charged particles were required to have acollinearity and acoplanarity above 60°. The smaller of the two momenta had to be below 70% of the greater one, and below 10 GeV/c.

For events with two reconstructed jets the scaled acoplanarity (see section 3.1) was required to be greater than 20°, the acoplanarity and the acollinearity greater 60°.

Lastly, events selected by the searches for acoplanar leptons or jets (sections 3.2 and 3.1) or the multiplepton search (section 3.4) were rejected. Figure 5 (e) shows the acoplanarity discribution for events passing the complete selection, in real data and simulated background.

3.6 Low transverse energy search

The low transverse energy (E_T) search was designed to complement the multilepton search for cascade decays or $\tilde{\chi}^0_2\tilde{\chi}^0_2$ production with low mass splitting where $\tilde{\chi}^0_2 \to \tilde{\chi}^0_1\ell^+\ell^-$. The first step of the selection was the same as for the multilepton search. In the second step, it was required that there be at least three and at most five charged particles, and that all such tracks had momenta above 500 MeV/c. Two or more of the charged particles had to satisfy stricter criteria on reconstruction and impact parameters.

In the third step, the highest and second highest momenta of charged particles were required to be below 50 and 25 GeV/c, respectively. At least one charged particle had to have a transverse momentum above 2.5 GeV/c, and at least one had to be an identified lepton. There had to be no neutral shower within 20° of the beam axis, and the second

highest jet energy must be below 30 GeV. Figure 5 (b) shows the distributions of $p_{\mathrm{T}}/\sqrt{s}$ for events fulfilling the above criteria in the real and simulated data.

This step was followed by the requirements that the polar angle of the total momentum had to satisfy $|\cos\theta_p| < 0.9$, and that the transverse energy of the event had to be greater than 4 GeV. The distributions of $M_{\mathrm{vis}}/\sqrt{s}$ for the real and simulated data, following the above selection, are compared in figure 5 (d).

The specific requirements for events with exactly two well reconstructed, isolated, charged particles were the same as in section 3.3, with the additional requirement that at least one of the tracks had to have have a momentum below 15 GeV/c.

Events with the transverse momentum exceeding 8 GeV/c, and the transverse energy greater than 10 GeV, where rejected, unless the scaled acoplanarity was above 20°.

Lastly, events selected by the searches for acoplanar leptons or jets (sections 3.2 and 3.1), the multiplepton search (section 3.4), or the tau cascade search (section 3.5) were rejected. Figure 5 (f) shows the distributions of scaled acoplanarity for real and simulated events, passing the complete selection.

4 Efficiencies and selected events

A total of 162000 $\tilde{\chi}^0_1\tilde{\chi}^0_2$ events was simulated for 42 different combinations of $M_{\tilde{\chi}^0_2}$ and $M_{\tilde{\chi}^0_1}$ masses with $M_{\tilde{\chi}^0_2}$ ranging from 25 GeV/c^2 to 180 GeV/c^2, and for different $\tilde{\chi}^0_2$ decay modes ($\mathrm{q\bar{q}}\tilde{\chi}^0_1$, $\mu^+\mu^-\tilde{\chi}^0_1$, $\mathrm{e^+e^-}\tilde{\chi}^0_1$, $\tilde{\tau}\tau$). A further 100000 $\tilde{\chi}^0_2\tilde{\chi}^0_{3,4,}$ events with cascade decays, were simulated for 56 different points. In addition, about $5{\cdot}10^8$ events were simulated using SGV in order obtain signal efficiencies for about 10^5 MSSM points.

Table 1 shows the number of events selected in the different searches in real data and the number expected from the SM background. Also shown are the main background sources contributing in each channel and the typical efficiency of each search for MSSM points where it is relevant. The main reason for the variation of the efficiencies is the variation of the masses of the particles involved in the process. The explicit rejection of events to avoid overlapping selections implies that the efficiencies are generally lower for those searches in which such rejection is performed (see section 3 and table 1).

Search	Data	Total bkg.	Main bkg.	Typical eff. (%)
Acoplanar jets	19	21.0±1.6	$\mathrm{W^+W^-}$,ZZ	10 – 30
Acoplanar electrons	16	20.7±3.7	$\mathrm{W^+W^-}$,$\gamma\gamma$	10 – 40
Acoplanar muons	16	14.6±1.3	$\mathrm{W^+W^-}$,$\gamma\gamma$	10 – 40
Multijets, γ:s	2	4.3±0.5	Zγ	10 – 20
Multijets, no γ:s	39	31.8±1.9	Zγ, $\mathrm{W^+W^-}$	10 – 40
Multileptons	23	28.2±1.2	$\mathrm{W^+W^-}$	30 – 50
Tau cascades	8	9.0±1.0	$\mathrm{W^+W^-}$,$\gamma\gamma(\rightarrow \mu^+\mu^-)$	13–19
Low E_T	18	19.0±3.3	$\gamma\gamma(\rightarrow \tau^+\tau^-)$	7–10

Table 1: Results of the different searches. The typical efficiency of each search for MSSM points where it is relevant is shown. The efficiencies depend typically on the masses of the sparticles involved in the process. For any given search, events are explicitly rejected if accepted by one of the searches appearing earlier in the table.

5 Results

In the absence of a signal for neutralino production, cross-section limits were derived using the dependence of the calculated efficiencies on the masses involved. The limits for the $\tilde{\chi}^0_1\tilde{\chi}^0_2$ production, as obtained from the searches for acoplanar leptons and jets, are shown in Figs. 6(a,b and c) assuming leptonic or hadronic decay modes. Similarly, Figs. 7(a,b) show cross-section limits for $\tilde{\chi}^0_2\tilde{\chi}^0_3$ production. For each mass combination, the limits were obtained by examining many possible (μ,M_2) points, for $\tan\beta = 1.1$ and high m_0, where $\tilde{\chi}^0_2\tilde{\chi}^0_3$ production was kinematically allowed. The point giving the worst limit was then taken. In the white regions marked "Not allowed" no such points were found. Fig. 7(a) shows the limit obtained using a bayesian combination[18] of the results from the multijet and acoplanar jet searches in the case where $\tilde{\chi}^0_3 \to \tilde{\chi}^0_2 q\bar{q}$ and $\tilde{\chi}^0_2 \to \tilde{\chi}^0_1 q\bar{q}$. Fig. 7(b) gives the corresponding limits when $\tilde{\chi}^0_2 \to \tilde{\chi}^0_1\gamma$, with $M_{\tilde{\chi}^0_2} - M_{\tilde{\chi}^0_1} > 10$ GeV/c^2, as obtained from the search for multijet events with a photon signature.

In addition to such limits on the production cross-sections the approach using a fast simulation makes it possible to scan regions of the MSSM parameter space and calculate the efficiencies and exclusion confidence level directly in each point, simulating contributing neutralino production channels and decay chains. Figs. 8 and 9 show the regions excluded by the different contributing searches in the (μ,M_2) plane for $\tan\beta = 1$ and $m_0 = 1$ TeV/c^2 and 80 GeV/c^2, respectively. Also shown are the combined exclusion regions for the two values of m_0, each obtained using the bayesian multi-channel approach [18]. In the region indicated as "Not allowed" the chargino is lighter than $\tilde{\chi}^0_1$. The τ cascade search is efficient when the chargino-neutralino mass difference is small, and for the cascade decays involving leptons in the region close to $\mu = 0$ at low m_0. The dotted line in the figures indicates the chargino isomass contour corresponding to the kinematic limit. The overall limit on $M_{\tilde{\chi}^0_1}$ for $\tan\beta = 1$ is determined by the intersection of this contour with the region excluded by neutralinos for high m_0 [1].

At low m_0 and low M_2, the region excluded by neutralinos shrinks with increasing $\tan\beta$, due to enhancement of the invisible $\tilde{\chi}^0_2 \to \tilde{\nu}\nu$, $\tilde{\nu} \to \nu\tilde{\chi}^0_1$ decay channel. There is no substantial change of the high m_0 exclusion region with the increase of $\tan\beta$.

6 Summary

Searches for neutralinos at $\sqrt{s} = 188.7$ GeV, using several mutually exclusive sets of criteria, gave no indications of a signal. As a consequence, preliminary limits on cross-sections for different topologies were derived, ranging from about 0.1 to several picobarn. The efficiencies computed with a full simulation of the DELPHI detector were extended to the whole range of the SUSY parameters explored by using a fast detector simulation, which included all neutralino production and decay channels. Preliminary exclusion regions in the MSSM parameter space were then derived. The methods used were designed for deriving general mass limits in the Minimal Supersymmetric Standard Model, as done in a separate note [1].

References

[1] DELPHI Coll., P.Andersson *et al.*, DELPHI-2000-031 CONF 350.

[2] P. Fayet and S. Ferrara, Phys. Rep. **32** (1977) 249;
H.P. Nilles, Phys. Rep. **110** (1984) 1;
H.E. Haber and G.L. Kane, Phys. Rep. **117** (1985) 75.

[3] DELPHI Coll., P. Abreu *et al.*, Phys. Lett. **B446** (1999) 75.

[4] DELPHI Coll., P. Abreu *et al.*, E. Phys. J. **C1** (1998) 1.

[5] A.Perrotta and N.Tinti, DELPHI 2000-004 PHYS 287.

[6] DELPHI Coll., P. Aarnio *et al.*, Nucl. Instr. and Meth. **303** (1991) 233;
DELPHI Coll., P. Abreu *et al.*, Nucl. Instr. and Meth. **378** (1996) 57.

[7] T. Sjöstrand, Comp. Phys. Comm. **39** (1986) 347;
T. Sjöstrand, `PYTHIA 5.6` *and* `JETSET 7.3`, CERN-TH/6488-92.

[8] DELPHI Coll., P. Abreu *et al.*, Z. Phys. **C73** (1996) 11.

[9] S. Katsanevas and P. Morawitz, Comp. Phys. Comm. **112** (1998) 227.

[10] J.E. Campagne and R. Zitoun, Z. Phys. **C43** (1989) 469.

[11] S. Jadach and Z. Was, Comp. Phys. Comm. **79** (1994) 503.

[12] F.A. Berends, R. Kleiss, W. Hollik, Nucl. Phys. **B304** (1988) 712.

[13] F.A. Berends, R. Pittau, R. Kleiss, Comp. Phys. Comm. **85** (1995) 437.

[14] J. Fujimoto *et al.*, Comp. Phys. Comm. **100** (1997) 128.

[15] S. Nova, A. Olshevski, and T. Todorov, in CERN Report 96-01, Vol. 2, p.224.

[16] R. Engel, Z. Phys. **C66** (1995) 203;
R. Engel and J. Ranft, Phys. Rev. **D54** (1996) 4244.

[17] M.Berggren, private communication, and
`http://home/cern/ch/~berggren/sgv.html`

[18] V.F. Obraztsov, Nucl. Instr. and Meth. **316** (1992) 388, *erratum* Nucl. Instr. and Meth. **399** (1997) 500.

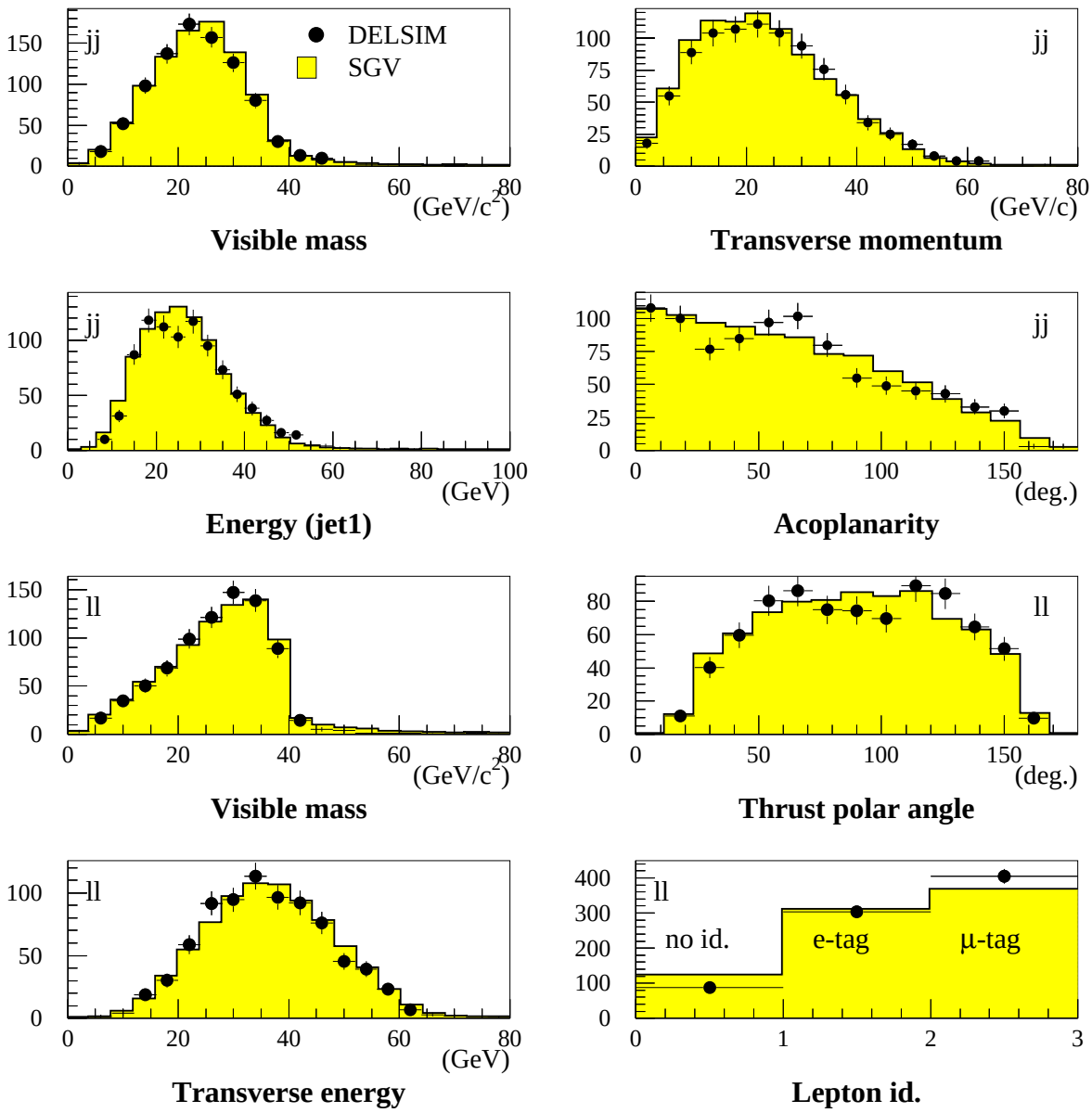

Figure 1: The expected distributions of relevant event variables characterising the $\tilde{\chi}_1^0\tilde{\chi}_2^0$ production with $M_{\tilde{\chi}_1^0} = 40$ GeV/c^2 and $M_{\tilde{\chi}_2^0} = 80$ GeV/c^2, as obtained using the full detector simulation (DELSIM) and SGV for the acoplanar jet (jj) and acoplanar lepton (ll) topologies. The decays $\tilde{\chi}_2^0 \to \tilde{\chi}_1^0 q\bar{q}$ or $\tilde{\chi}_1^0 \ell^+\ell^-$ were assumed as appropriate ($\ell^+\ell^-$ denotes e^+e^- and $\mu^+\mu^-$ in equal proportions).

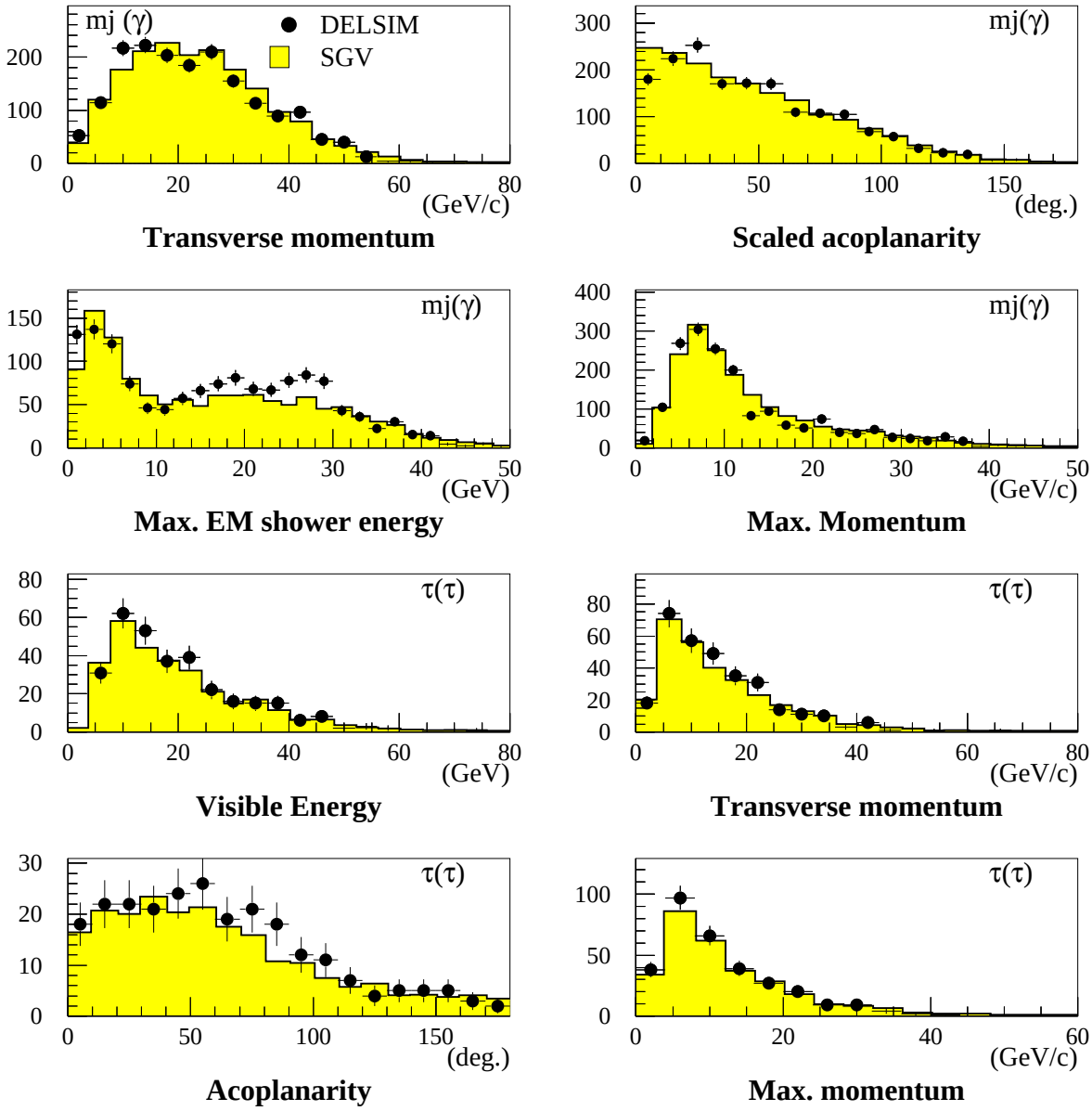

Figure 2: The expected distributions of relevant event variables characterising the $\tilde{\chi}_1^0\tilde{\chi}_2^0$ production for the multijet topologies (top) and the asymmetric taus topology. In the multijet case chosen $\tilde{\chi}_4^0\tilde{\chi}_2^0$ production dominates with 50% of the $\tilde{\chi}_2^0$:s decaying to $\tilde{\chi}_1^0\gamma$. The neutralino masses are $M_{\tilde{\chi}_1^0} = 31$ GeV/c^2, $M_{\tilde{\chi}_2^0} = 60$ GeV/c^2, and $M_{\tilde{\chi}_4^0} = 100$ GeV/c^2. In the asymmetric tau case $\tilde{\chi}_1^0\tilde{\chi}_2^0$ production with $\tilde{\chi}_2^0 \to \tau\tilde{\tau} \to \tau\tau\tilde{\chi}_1^0$ was assumed. The relevant masses were $M_{\tilde{\chi}_1^0} = 34.8$ GeV/c^2, $M_{\tilde{\tau}} = 36.8$ GeV/c^2, and $M_{\tilde{\chi}_2^0} = 60$ GeV/c^2.

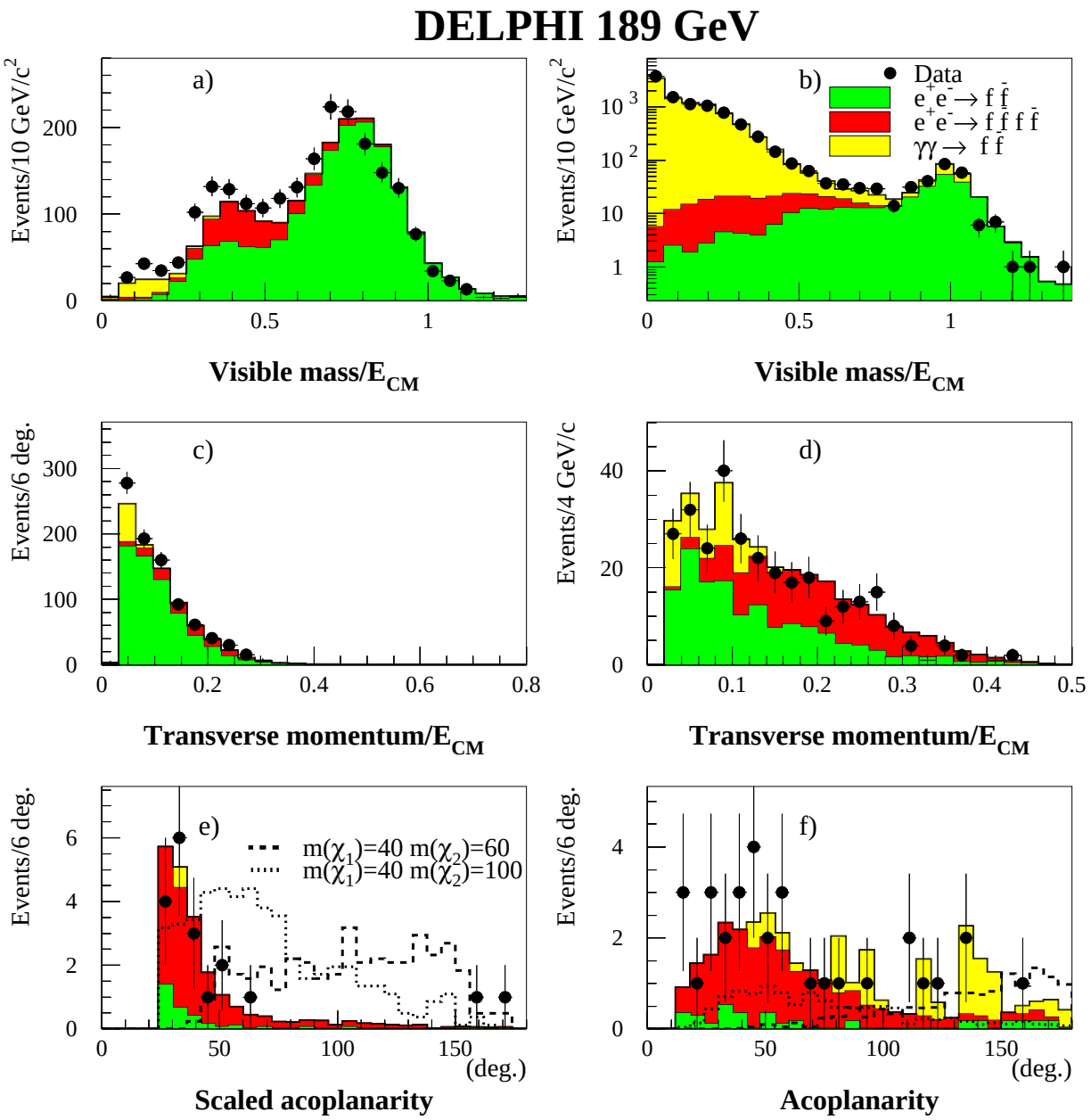

Figure 3: The comparison between the real and simulated data for the acoplanar jet selection (a,c,e) and acoplanar lepton selection (b,d,f) is shown. Plots (a,b) show the visible mass divided by the centre-of-mass energy at an initial stage of the selections. Plots (c,e) shows the missing transverse momentum divided by centre-of-mass energy at an intermediate stage of the selections. Plots (e,f) show acoplanarity distributions after the last step of the selections, where in addition, the expected signal of of $\tilde{\chi}_1^0\tilde{\chi}_2^0$ production for two different neutralino mass combinations, is also shown. The signal was normalized to a cross-section of 1 pb and the decay $\tilde{\chi}_2^0 \to Z^*\tilde{\chi}_1^0$ was assumed. The selections are described in sections 3.1 and 3.2.

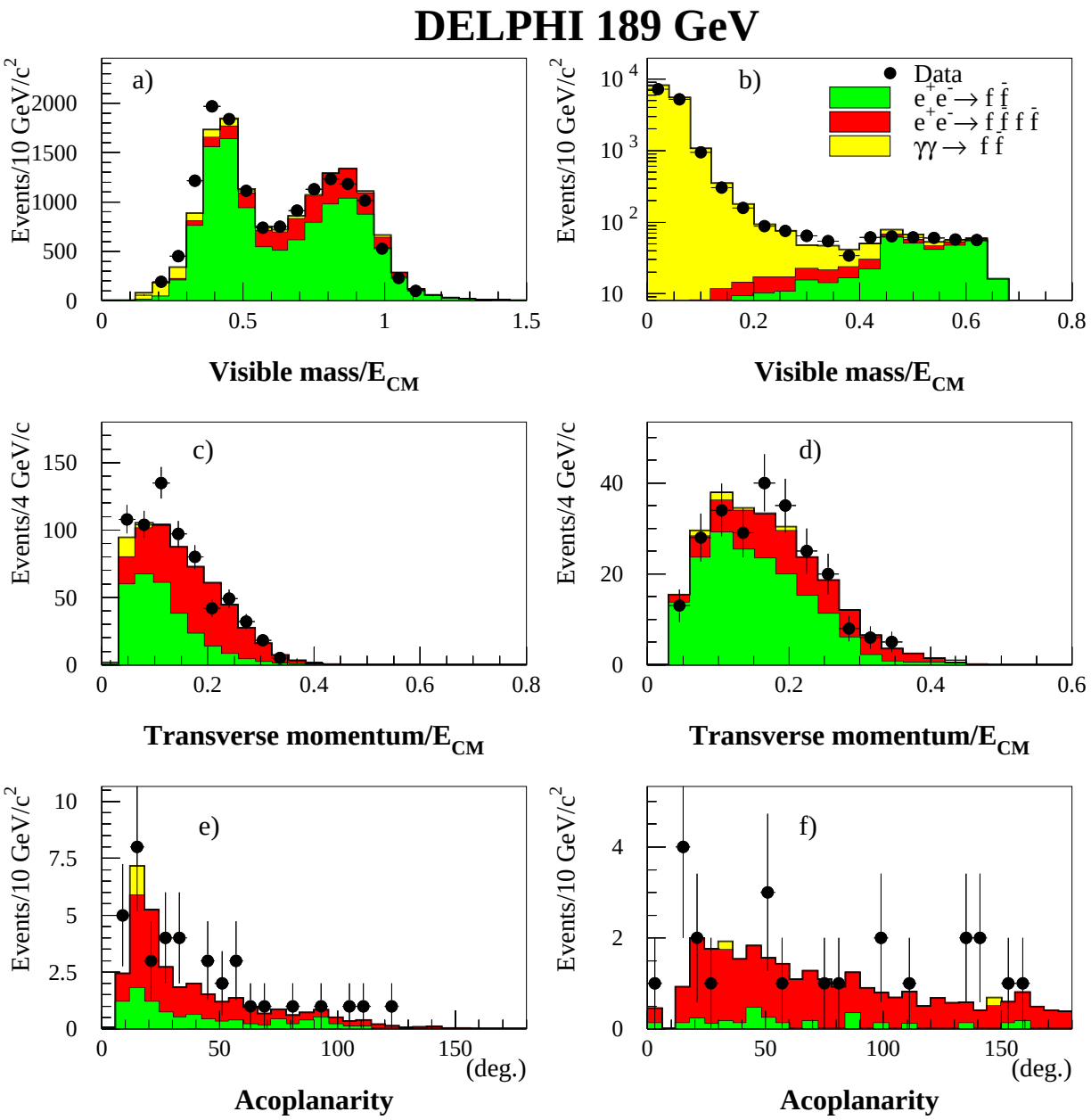

Figure 4: The comparison between the real and simulated data for the multijet selection (a,c,e) and multilepton selection (b,d,f) is shown at three different stages of the selection. Plots (a,b) show the $M_{\rm vis}$ divided by the centre-of-mass energy at an initial stage of the selections. Plots (c,d) show the missing transverse momentum at an intermediate stage of the selections, while the plots (e,f) show the acoplanarity after the last step of the selections. The selections are described in sections 3.3 and 3.4.

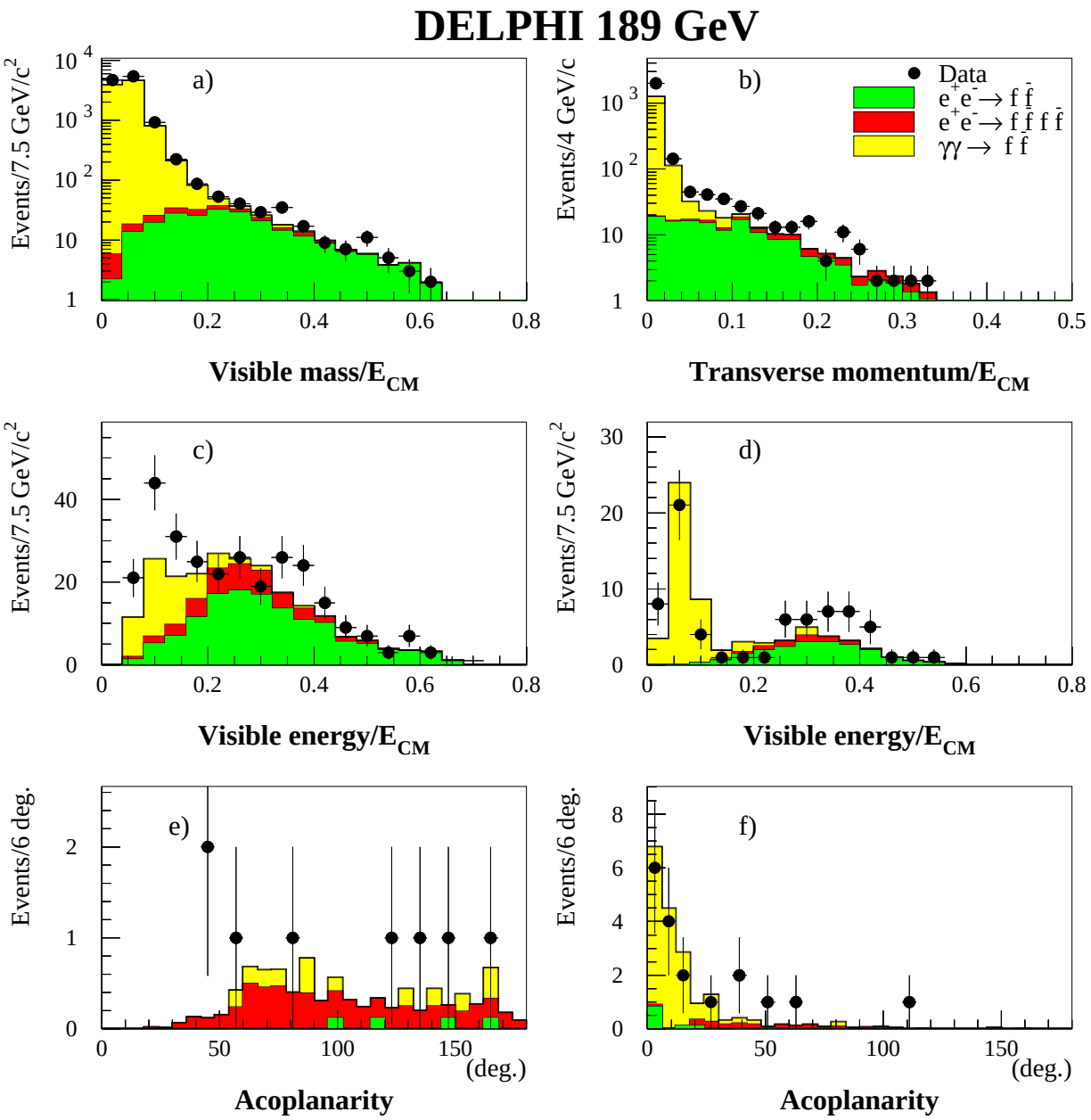

Figure 5: The comparison between the real and simulated data for the asymmetric tau selection (a,c,e) and low E_T selection (b,d,f) is shown. Plots (a,b) show the $M_{\rm vis}$ divided by the centre-of-mass energy and transverse momentum divided by the centre-of-mass energy at an initial stage of the selections. Plots (c,d) show the visible energy divided by the centre-of-mass energy at an intermediate stage of the selections and plots (e,f) show the acoplanarity after the last step of the selections. The selections are described in sections 3.5 and 3.6.

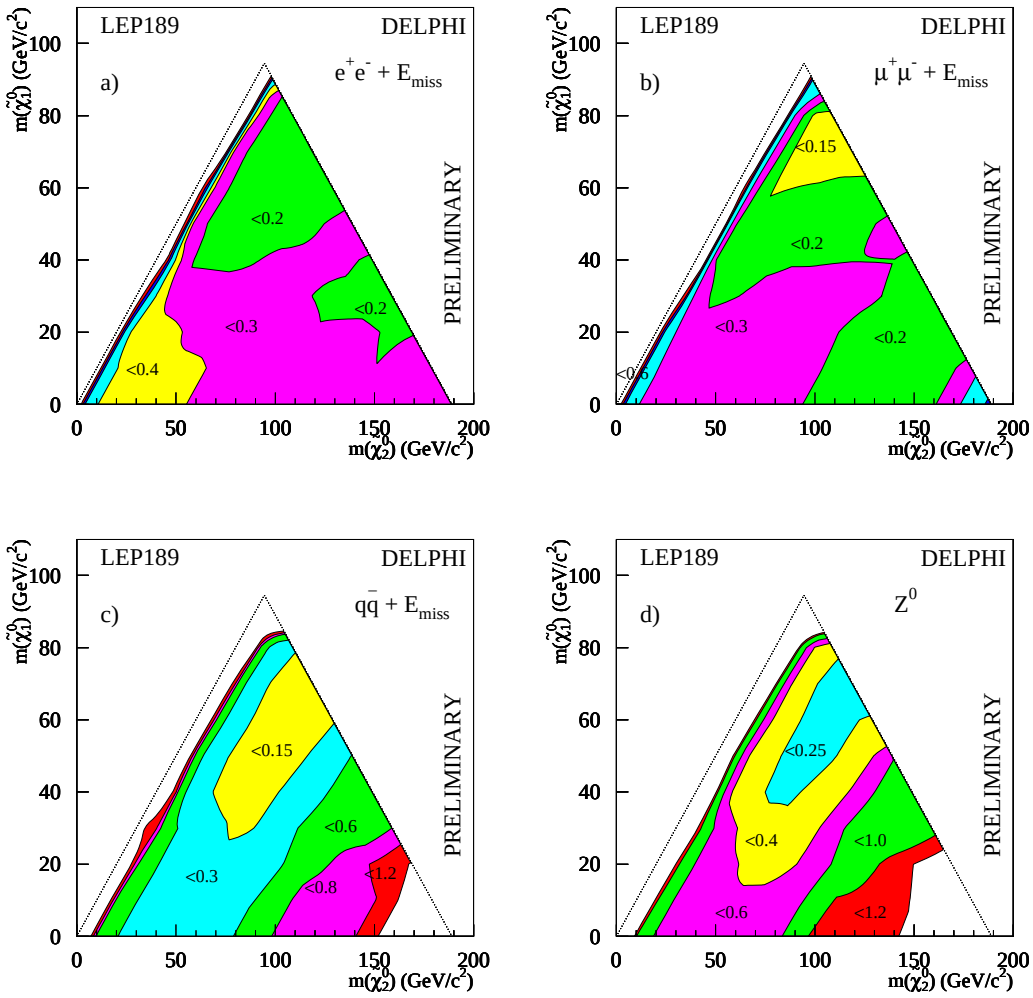

Figure 6: Contour plots of upper limits on the cross-sections at the 95% confidence level for $\tilde{\chi}^0_1\tilde{\chi}^0_2$ production at $\sqrt{s} = 189$ GeV. In each plot, the different shades correspond to regions where the cross-section limit in picobarns is below the indicated number. For figures a), b), c), $\tilde{\chi}^0_2$ decays into $\tilde{\chi}^0_1$ and a) e^+e^-, b) $\mu^+\mu^-$, and c) $q\bar{q}$, while in d) the branching ratio of the Z was assumed, including invisible states. The dotted lines indicate the kinematic limit and the defining relation $M_{\tilde{\chi}^0_2} > M_{\tilde{\chi}^0_1}$.

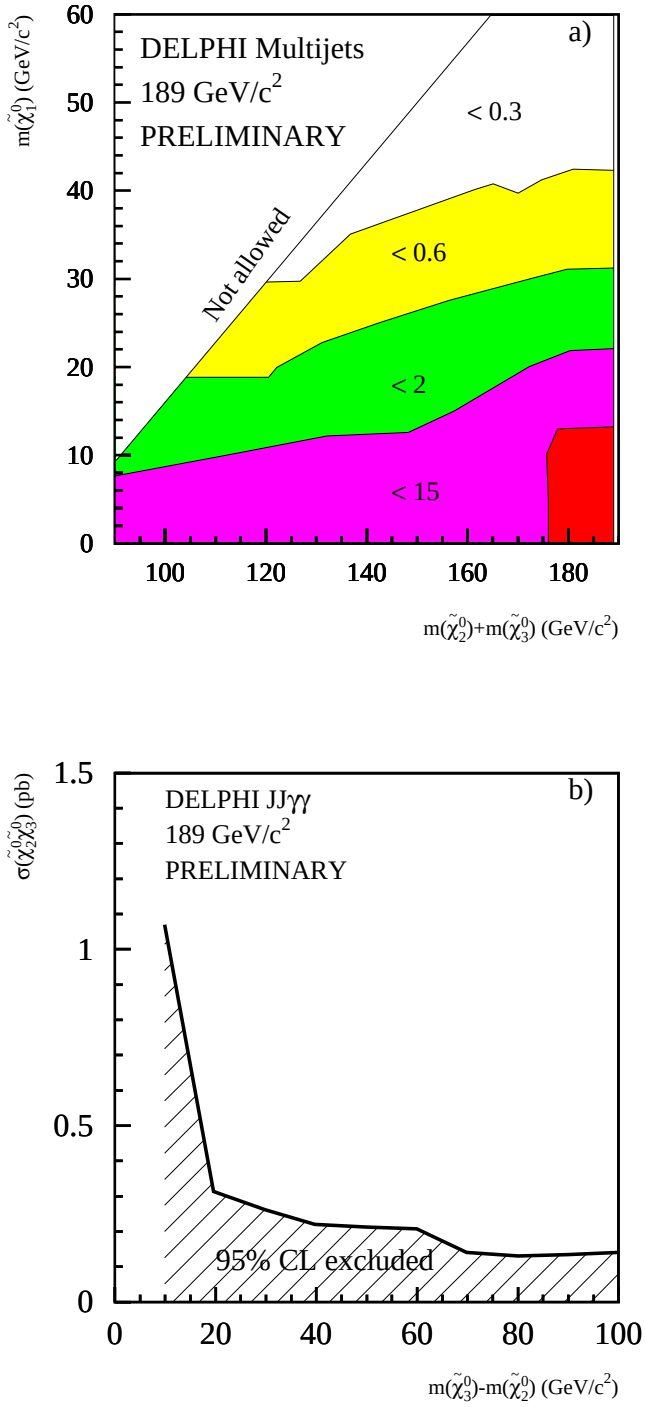

Figure 7: Upper limits on the cross-sections at the 95% confidence level for $\tilde{\chi}_2^0\tilde{\chi}_3^0$ production at $\sqrt{s} = 189$ GeV. In upper plot, the different shades correspond to regions where the cross-section limit in picobarns is below the indicated number. In a) the branching ratio of $\tilde{\chi}_2^0$ to $\tilde{\chi}_1^0\gamma$ was set to zero, while in b) it was one. In b) it was also assumed that $M_{\tilde{\chi}_2^0} - M_{\tilde{\chi}_1^0} > 10$ GeV/c^2. Similar limits apply in the case of $\tilde{\chi}_3^0\tilde{\chi}_4^0$ production.

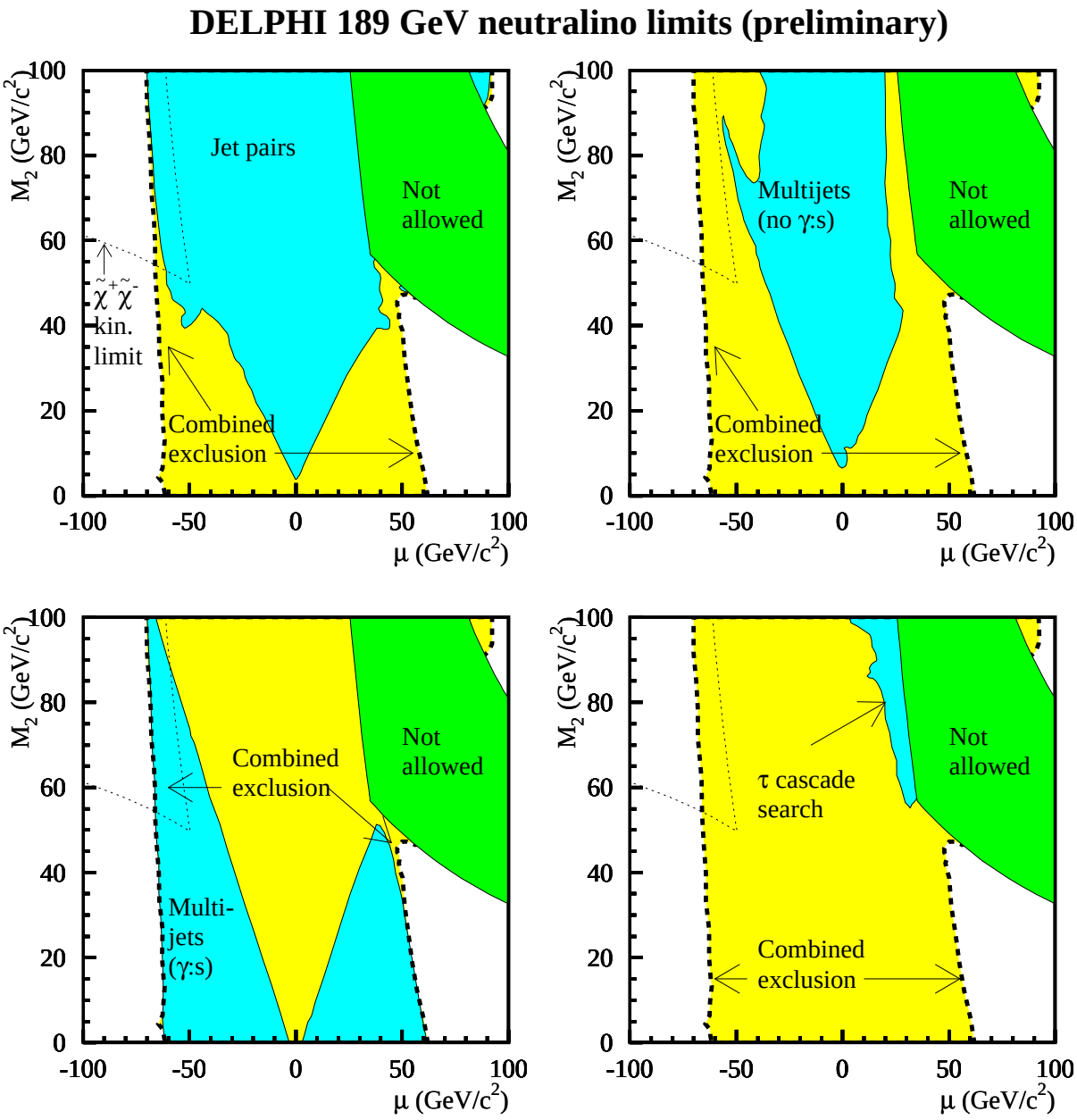

Figure 8: Regions in the (μ, M_2) plane excluded at 95% confidence level for $\tan\beta$=1, assuming $m_0 = 1$ TeV/c^2. Four regions excluded by different contributing searches are compared with the combined exclusion (thick dashed curve) and the kinematic limit for chargino production.

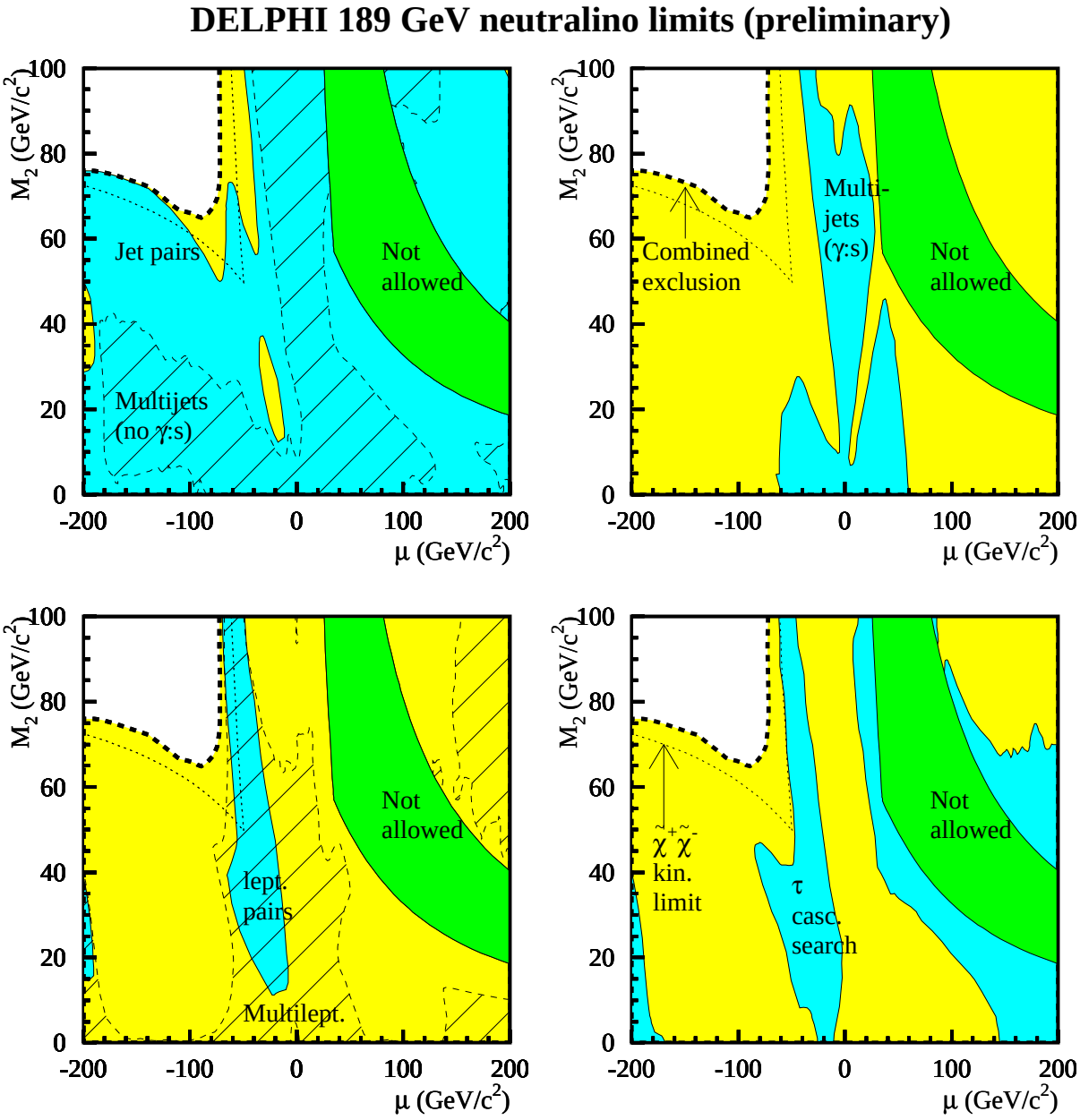

Figure 9: As figure 8, but for $m_0 = 80$ GeV/$c^2$and six different contributing searches. The hatched areas are excluded by the multijet and multilepton searches.